Derivation of Surface Soil Water Content Using a Simplified Geometric Method in Allahabad District, Uttar Pradesh India

Abba Aliyu Kasim

Abstract- Surface soil water content (surface moisture availability) is the principal indicator of soil physical fertility. A simplified geometric method is presented for estimating surface soil water content in Allahabad district using remotely sensed multispectral satellite data (Landsat 7ETM+). Surface radiant temperature and Normalized Difference Vegetation Index (NDVI)/Fractional vegetation cover were derived from optical/thermal satellite imagery. The method utilizes the relationship between these satellite measurements to infer surface soil water content. The derived surface soil water content values were correlated with ground measured volumetric soil water content. A poor correlation coefficient was found to exist (R2 < 0.2) on all the dates under study, presumably indicating that soil surface water content has become decoupled from the soil water content at deeper layers. Surface soil water content maps were created to show spatial and temporal variability in surface soil water content in Chaka block (sub-study area). The merit of this method is that it does not require any other parameters (surface data or model output), however, it has great potential to work as any other more sophisticated approach for estimating surface soil water content.

Key words: Simplified Geometric Method, Surface Soil Water Content, Fractional Vegetation Cover, Surface Radiant Temperature

1. INTRODUCTION

Adequate information of surface soil water content is essential in many spheres of knowledge such as climatology, meteorology, agriculture, hydrology, ecology and biogeochemistry. Hence, proper monitoring of surface soil water content over large areas is necessary for efficient agricultural managements and crop drought forecasting [13]. Surface soil water content varies greatly in time, depth and space. The key soil properties that influence the amount of moisture present in the soil include: soil texture, soil organic matter content and soil structure [6],[1]. Soil moisture can be measured using various techniques ranging from crude to more sophisticated and advanced procedures. Das [12] explained some of the important techniques for measuring soil moisture which include: gravimetric method, electrical conductivity method, neutron scattering method and measurement using tensiometers.

- *Corresponding Author: Abba Aliyu Kasim, M Sc. Student, Department of Soil Water, Land Engineering & Management, Sam Higginbottom Institute of Agriculture, Technology & Sciences, Allahabad - 211007, U.P., India. Email: abbaaliyukasim@yahoo.com*

It is a proven fact that geospatial technology (Remote sensing and GIS) has capability of estimating and mapping land surface parameters such as surface moisture availability and evapotranspiration. Microwave remote sensing (active and passive) and optical/thermal IR remote sensing are promising techniques for estimating surface soil water content. Optical/thermal IR remote sensing for estimating soil moisture (Triangle Method) uses land surface temperature (LST) and vegetation index such as Normalized Difference Vegetation Index (NDVI); Enhanced Vegetation Index (EVI) derived from optical/thermal imageries to infer moisture availability in a target. The basic idea of this method is that spatial inhomogeneity in surface soil wetness is implied by variations in surface radiant temperature [6],[7],[23],[14].

Carlson, [8] presented a new and simple geometric method to obtain land surface parameters (soil water content and evapotranspiration). This method is a variant of the famous triangle model. The great advantage of this method is that it does not require any surface data or model output to find the solution of the model equation and it works like sophisticated and complex numerical simulations.

2. MATERIAL AND METHODS

2.1.1. Study Area

Allahabad is situated in the southern part of the Uttar Pradesh (UP), India. It stands at the confluence of the sacred Ganga, Yamuna and the invisible Saraswati rivers. Allahabad is enclosed between latitude 25.45°N and longitude 81.84° at an elevation of 98 meters (322 ft.) above mean sea level [3]. Six (6) Tehsils (geographical areas) were chosen for the study. These are Karchhana, Phulpur, Bara, Koraon, Soraon and Handia. Chaka Block (sub-study area) which is situated within the Karchhana Tehsil was selected as soil sampling site.

The typical climate of Allahabad is humid subtropical climate denoted as *Cwa* in the Köppen climate classification. The annual rain is about 1027mm. The temperature ranges from 40°C to 45°C and from 20^0C to 24^0C during summer and winter respectively [3],[4].

The soils of Allahabad district were developed under the synergistic impacts of a wide range of soil forming factors including climate, vegetation and parent materials. The area is covered by layers of alluvium spread by the slow-moving rivers of the Ganges system [19]. Alluvial soils are the most fertile soils among all Indian soils [18]. Chaka block has moderately shallow and eroded loamy soils [2], [22]. The vegetation of the study site consists mainly of scrub. Forests lie in Trans-Yamuna and some portions of the Vindhya Hills.

2.1.2. Dataset Description

Landsat 7 Enhanced Thematic Mapper Plus data was utilized in this paper. The ETM+ sensor aboard Landsat 7 image consists of 8 spectral bands (blue, green, red, near-infrared, shortwave infrared, thermal infrared and panchromatic).

Landsat 7 ETM+ data (Path/Row 143/42) was procured from United States Geological Survey (USGS) site (http://glovis.usgs.gov). The acquisition dates of the images are 30th January, 2015; 15th February, 2015; 19th March, 2015; 20th, April, 2015 and 06th May, 2015. The images of 3rd March, 2015 and 4th April were very cloudy.

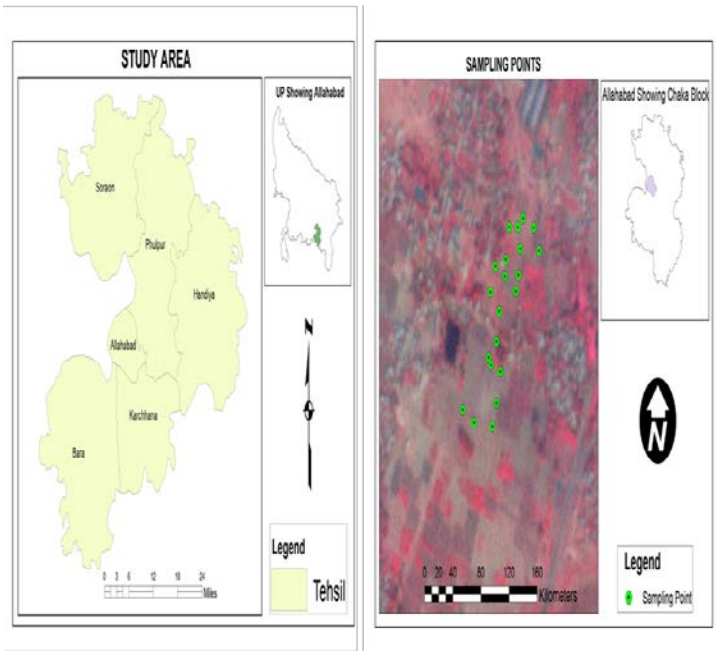

Figure 1: Study Area and Sampling Points

2.1.3. In situ Measurements

Soil samples were collected at some locations (22 sampling points) in the Chaka Development Block area at two depths (0-5cm and 5-15cm). The Landsat 7 ETM+ overpass time is 5:00 am GMT which corresponds to 10:30am Indian time. Therefore, soil sampling was carried out between 10:30 and 11:30am (local time of India). Gravimetric method was used to determine the moisture content using the procedures explained in [18].

2.1.4. Methodology

2.1.5. Pre-processing and Processing Operations of Satellite Imagery

The quantized calibrated pixel value (DN) was converted to at-sensor spectral radiance according to procedures given by [10].

$$L_\lambda = \left(\frac{LMAX_\lambda - LMIN_\lambda}{Qcalmax - Qcalmin}\right)(Qcal - Qcalmin) + LMIN_\lambda \quad (1)$$

Where:

L_λ= Spectral radiance at the sensor's aperture [W/ (m^2 sr µm)]; Q_{cal} = Quantized calibrated pixel value [DN];Qcalmin = Minimum quantized calibrated

pixel value corresponding to LMINλ [DN];Qcalmax = Maximum quantized calibrated pixel value corresponding to LMAXλ [DN];

$LMIN_\lambda$=Spectral at-sensor radiance that is scaled to Qcalmin [W/(m² sr µm)]; $LMAX_\lambda$= Spectral at-sensor radiance that is scaled to Qcalmax [W/(m2 sr µm)].

The at-satellite band reflectance (BD) was computed from at satellite directional radiance as follows: [15],[21],[10].

$$\boldsymbol{\rho_{t,b}} = \frac{\boldsymbol{\pi.L_{t,b}.d^2}}{\boldsymbol{ESUN_b\ .\cos\theta rel}} \qquad (2)$$

Where:

$\rho_{t,b}$ is at-satellite band reflectance (BD)/ Planetary TOA reflectance [unitless]; π is mathematical constant equal to ~3.14159 [unitless]; $L_{t,b}$ is at-satellite spectral radiance in band b (W m-2 sr-1 µm-1); $ESUN_b$ is the mean solar exoatmospheric radiation over band b (W m^{-2} sr-1 µm-1); Θrel is solar incident angle or solar zenith angle relative to the land surface slope and d^2 is earth-sun distance in astronomical unit. The parameter d^2 is computed as the function of day of year using the following equation: [21],[10].

$$d^2 = \frac{1}{1+0.033\cos(DOY.2\pi/365)} \qquad (3)$$

Where DOY is day of year and (D0Y. 2π/365) (rad).

2.1.6. Derivation of Normalized Difference Vegetation Index (NDVI) and Fractional Vegetation Cover

NDVI which is a function of the surface derived reflectance in the Red and NIR bands was calculated using the following formula:

$$NDVI = \frac{\rho_{nir}-\rho_{red}}{\rho_{nir}+\rho_{red}} \qquad (4)$$

Where: ρ_{nir} is reflectance in the near-infrared band; ρ_{red} is reflectance in the red band.

Fractional vegetation cover was derived from the scaled NDVI (N*).

$$Fr = N^{*2} \qquad (5)$$

Where scaled NDVI (N*) is calculated using the following formula as:

$$N^* = \frac{NDVI-NDVI_0}{NDVI_{max}-NDVI_0} \qquad (6)$$

$NDVI_0$ is the value corresponding to bare soil and $NDVI_{max}$ is the value corresponding to the full vegetation [5].

2.1.7. Derivation of Emissivity Corrected Surface Radiant Temperature

The surface emissivity can be incorporated into thermal atmospheric correction of thermal remotely sensed data so as to determine accurate radiometric temperatures [5]. Therefore, surface emissivity was computed so as to incorporate it into land surface temperature derivation algorithm.

$$\boldsymbol{T} = \frac{\boldsymbol{K_2}}{\boldsymbol{\ln(\frac{K_1*\varepsilon}{CV_{R1}}+1)}} \qquad (7)$$

Where: T is in degrees Kelvin. It can be converted to degree Celsius by subtracting 273.15 from the kelvin values.

K_1 and K_2 are calibration constants for Landsat 7 ETM+ equal to 666.09 W m^{-2} sr^{-1} μm^{-1} and 1282.71 W m^{-2} sr^{-1} μm^{-1} respectively ([10],[16].

CV_{RI} (L_λ) is cell value as radiance (W m^{-2} sr^{-1} μm^{-1}); ε is surface emissivity [unitless] computed using (8).

$$\boldsymbol{\varepsilon_i = Fr.\varepsilon_v + (1-Fr).\varepsilon_s} \qquad (8)$$

Where: Fr is fractional vegetation cover; ε_i is pixel's emissivity; ε_v is emissivity of vegetation; ε_s is emissivity of soil.

2.1.8. Scaling NDVI and Surface Radiant Temperature

The NDVI was scaled using the formula discussed above in (6). Surface radiant temperature was also scaled likewise according to [7] algorithm.

$$\boldsymbol{T^*} = \left\{\frac{(\boldsymbol{T_{ir}-T_{min}})}{(\boldsymbol{T_{max}-T_{min}})}\right\} \qquad (9)$$

Where: T_{ir} is surface radiant temperature; $T_{min}$is minimum temperature in the image; T_{max} is maximum temperature in the image. Both the scaled NDVI and T* values range from 0 to1.

2.1.9. Creation of T*-Fr Triangular Space

A scatter plot of Fr versus scaled surface radiant temperature was developed for each date in order to observe the triangle. The Fr was plotted on ordinate while the scaled surface radiant temperature on abscissa. An algorithm was used to fit the warm edge according to [17] procedure.

$$\mathbf{T^*_{max(i)} = a + bFr_i} \qquad (10)$$

Where: Fr_i is the fractional vegetation cover of pixel i-th pixel; a is the intercept of the linear warm edge; b is the slope of the linear warm edge.

2.1.10. Transformation of Pixel Measurements into Surface Moisture Availability

Pixel measurements were transformed into surface moisture availability using a simplified geometric algorithm. The inputs of the algorithm are fractional vegetation cover and scaled surface radiant temperature.

$$\mathbf{Mo} = \frac{\mathbf{1 - T^*(pixel)}}{\mathbf{T^*_{warm\ edge}}} \qquad (11)$$

Where:

$T^*_{warm\ edge} = (1 - Fr); Mo \leq 1.0; \geq 0.$

3. RESULTS AND DISCUSSION

3.1.1. Triangular Space of T* versus Fr

The pixel distribution on the scatter plots forms triangular shapes on each date under study (figure 2). This is because the range of surface radiant temperature decreases as the amount of vegetation cover increases and sufficient number of pixels exists. The warm edge is the right edge of the distribution and the left edge is defined as the wet (cold) edge. The pixels along warm edge have higher surface radiant temperature owing to low evaporation rates from dry soils under low vegetation condition or low transpiration rates from vegetation canopy under high ground vegetation cover which in turn causes stomatal closure in the canopy. Pixels along cold edge have cool surface temperature. This is because of high evaporation rates from wet soils under low vegetation condition or high transpiration from vegetation canopy under high vegetation condition which indicates the presence of high amount of moisture and lack of water stress. These findings are in accord with the interpretation of triangular space by [7],[23],[11],[20]. By locating where a pixel falls in the triangle in a particular day and finding its position in the next successive days, a trajectory is formed which explains the drying or wetting process. An Algorithm was used to fit the warm edge. This is very useful when the triangle is not pronounced.

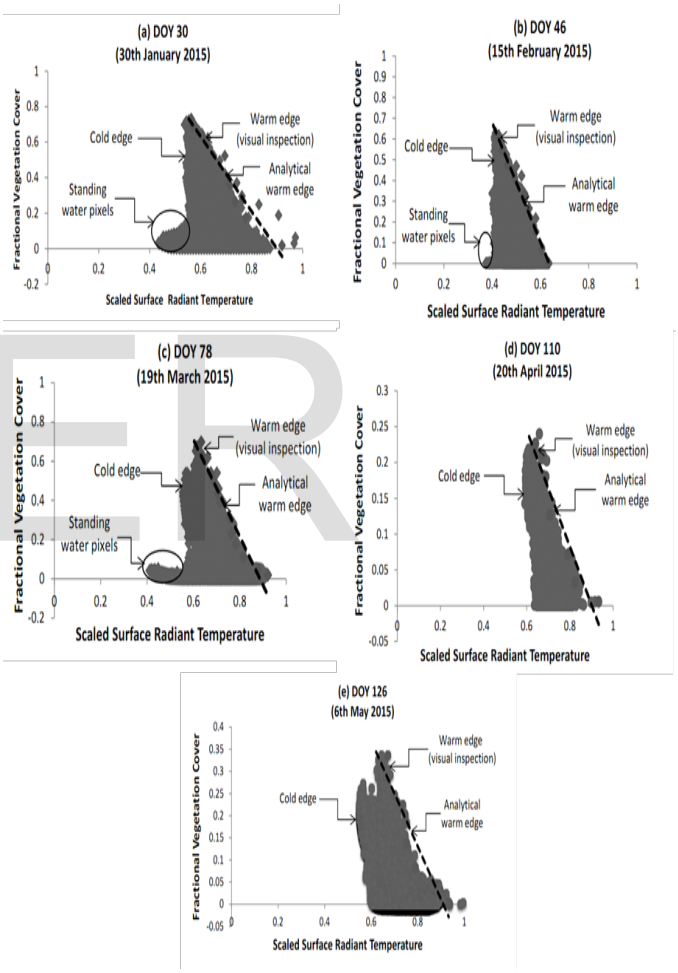

Figure 2: Triangular Space of Scaled Surface Radiant Temperature versus Fractional Vegetation Cover (Before removal of standing water pixels)

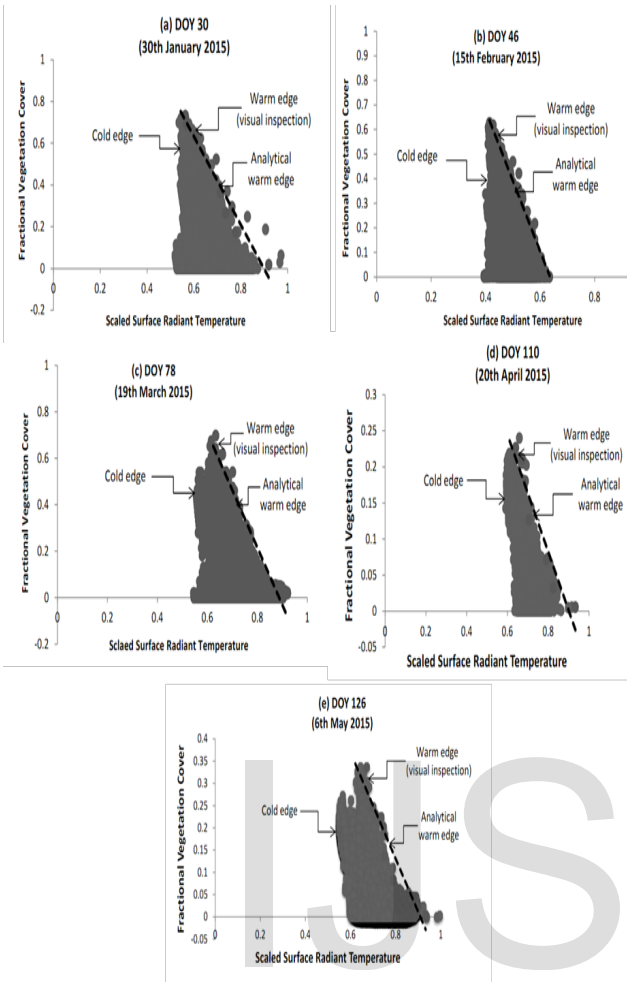

Figure 3: Triangular Space of Scaled Surface Radiant Temperature versus Fractional Vegetation Cover (After removal of standing water pixels)

The cloud and water pixels distort the shape of the triangle around the boundaries. It is very noticeable in the triangles of the 30th January, 2015 (DOY 30), 15th February, 2015 (DOY46) and 19th March, 2015 (DOY 78) that the triangles bulge in the lower left side. This distortion is likely to be caused by standing water pixels because of lower reflectivity and a bit higher temperature of water in comparison with cloud. These distortions are removed in figure 3.

3.1.2. Spatial and Temporal Distribution of Surface Soil Moisture

Surface moisture availability tends to vary spatially owing to the certain factors such as the nature of the scenery, soil type, land use, occurrence of the hydrological events et cetera. Chaka block in Allahabad was chosen to depict the spatial variation of simulated surface soil moisture. The findings have shown that surface soil moisture varied spatially and temporally within the area under investigation. Figure 4 shows the spatial variability maps of simulated soil moisture at 30m resolution using geometric method algorithm between the study dates. The range of soil moisture decreases progressively between DOY 46 and DOY 110. This might be as a result of the absolute cessation of rainfall between March and April.

3.1.3. Correlation Analysis

The simulated soil moisture using the geometric model algorithm was correlated with ground measured volumetric soil moisture at depths 5cm and 15cm. The findings showed a very weak correlation between the simulated surface soil moisture and ground measured soil moisture at deeper soil layers (Table 1). This indicated that triangle models can only estimate soil moisture content at the superficial layer of the soil. Therefore, it is a salient consideration when the method is being applied.

The possible reason of poor correlation between modeled and measured surface soil water content can be attributed to the depth at which soil moisture measurements were made. To identify the possible reason(s) for the poor correlation between modeled and estimated soil moisture in the present study, series of personal communications were made with the developer of the algorithm/model in May 2015 (Professor Toby N. Carlson, Penn State University, USA) [9]. According to the developer it might be difficult to get a good agreement between ground measured soil moisture at deeper substrate and estimated surface soil water content (using triangle method) as the latter technique estimates moisture availability at the top skin layer of the soil (0.5 to 1cm).

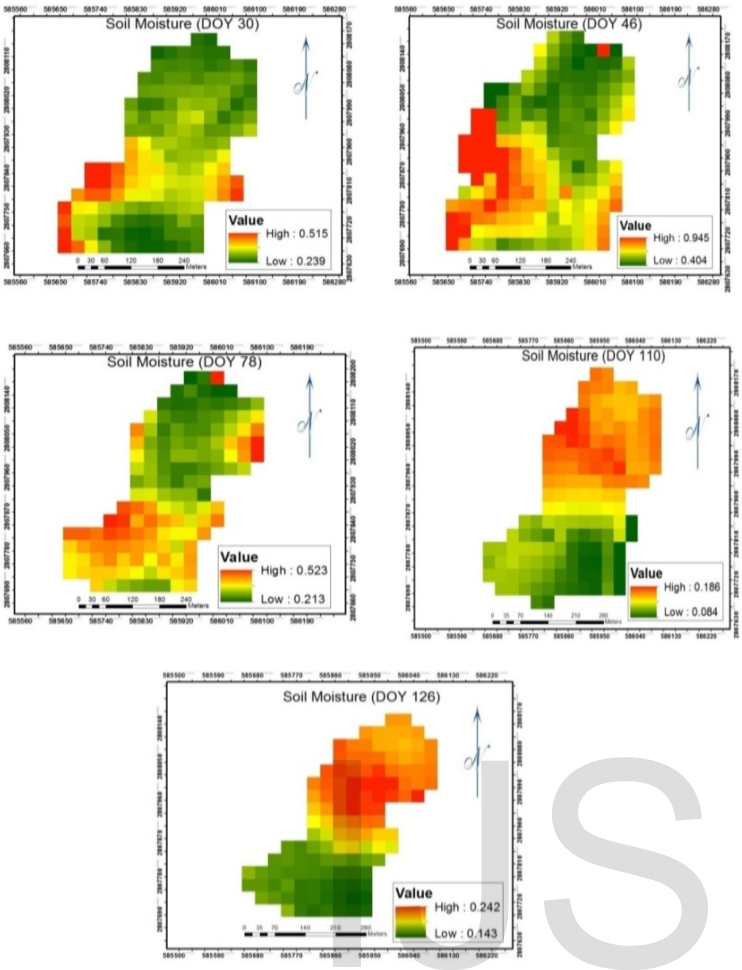

Figure 4: Spatial Distribution Maps of Simulated Surface in Chaka Block

Table 1: Correlation Coefficient (R^2) between Simulated Surface Moisture and Ground Measured Volumetric Water in Chaka Block

S. No.	Date	Geometric Method Algorithm	
		SM (5 cm)	SM (15 cm)
1	30th Jan, 15	0.0238	0.0057
2	15th Feb, 15	0.1184	0.0097
3	19th Mar, 15	0.0168	0.0001
4	20th Apr, 15	0.0651	0.1099
5	06th May, 15	0.1352	0.145

4. CONCLUSIONS

In conclusion, this study estimated the surface soil water content using the relationship between surface radiant temperature and fractional vegetation cover derived from satellite imagery (simplified geometric method). The modeled and actual volumetric soil moisture correlated poorly. This poor correlation can be attributed to the depth at which soil moisture measurements were made (5cm and 15cm). Hence, this technique is more suitable and efficient for estimating soil moisture at the superficial soil layer (0.5-1cm).

Acknowledgment

The author would like to express his indebtedness to Professor Emeritus Toby Nahum Carlson of Penn State University, USA for his precious advice and help.

References

[1] Adam, G. K., & Aliyu, A. K. (2012). Determination of the Influence of Texture and Organic Matter on Soil Water Holding Capacity in and Around Tomas Irrigation Scheme, Dambatta Local Government Kano State. Research Journal of Environmental and Earth Sciences, 4(12): 1038-1044.

[2] Agriculture Contingency Plan for District: Allahabad. (2015, 08 10). Retrieved August Monday, 2015, from http://agricoop.nic.in/Agriculture%20Contingency%20Plan/UP/UP62-Allahabad-28.07.14.pdf

[3] Allahabad Profile. (2015, 08 10). Retrieved August Monday, 2015, from http://allahabad.nic.in/geostructure.htm

[4] Allahabad Wikipedia. (2015, 08 31). Retrieved August Monday, 2015, from Wikipedia: https://en.wikipedia.org/wiki/Allahabad

[5] Brunsell, N. A., & Gillies, R. R. (2002, December). Incorporating surface emissivity into a thermal atmospheric correction. Photogrammetric Engineering & Remote Sensing, 68, 1263–1269.

[6] Capehart, W. J., & Carlson, T. N. (1997). Decoupling of surface and near-surface soil water content: A remote sensing perspectiv. Water Resources Research, 33(6), 1383-1395.

[7] Carlson, T. N. (2007). An overview of the "triangle method" for estimating surface evapotranspiration and soil moisture from satellite imagery. Sensors, 7, 1612-1629.

[8] Carlson, T. N. (2013). Triangle models and misconceptions. International Journal of Remote Sensing Applications, 3 (3).

[9] Carlson, T. N. (2015, May Saturday). Personal communicationtion by email. (A. K. Aliyu, Interviewer)

[10] Chander, G., Markham, B. L., & Helder, D. L. (2009). Summary of current radiometric calibration coefficients for Landsat MSS, TM, ETM+,and EO-1 ALI sensors. Remote Sensing of Environment, 113, 893–903.

[11] Chen, C.-F., Son, N.-T., Chang, L.-Y., & Chen, C.-C. (2011). Monitoring of soil moisture variability in relation to rice cropping systems in the Vietnamese Mekong Delta using MODIS data. Applied Geography, 31, 463-475.

[12] Das, D. K. (2011). Introductory soil science. New Delhi: Kalyani publishers.

[13] Feng, Z., Li-Wen, Z., Jing-Jing, S., & Jing-Feng, H. (2014). Soil moisture monitoring based on land surface temperature-vegetation index space derived from MODIS data. Pedosphere, 24 (4), 450–460.

[14] Haas, J. (2010). Soil moisture modelling using TWI and satellite imagery in the Stockholm region. Stockholm, Sweden.

[15] LPSO. (2006). The Landsat 7 Science Data User's Handbook. Maryland: NASA's Goddard Space Flight Center Greenbelt.

[16] Mallast, U., Gloaguen, R., Friesen, J., Rödiger, T., Geyer, S., Merz, R., et al. (2014). How to identify groundwater-caused thermal anomalies in lakes based on multi-temporal satellite data in semi-arid regions. Hydrol. Earth Syst. Sci., 18, 2773–2787.

[17] Mallick, K., Bhattacharya, B. K., & Patel, N. (2009). Estimating volumetric surface moisture content for cropped soils using a soil wetness index based on surface temperature and NDVI. Agricultural and Forest Meteorology, 149 (2009), 1327–1342.

[18] Methods Manual, Soil Testing in India . (2011 , January). New Delhi , India: Department of Agriculture & Cooperation Ministry of Agriculture Government of India .

[19] National Disaster Risk Reduction Portal . (2015, 08 10). Retrieved August Monady, 2015, from http://nidm.gov.in/pdf/dp/Uttar.pdf

[20] Shafian, S., & Maas, S. J. (2015). Improvement of the trapezoid method using raw landsat image digital count data for soil moisture estimation in the Texas (USA) high plains. Sensors, 15, 1925-1944.

[21] Tasumi, M., Allen, R. G., & Trezza, a. R. (2008). At-Surface reflectance and albedo from satellite for operational calculation of land surface energy balance. Journal of Hydrologic Engineering, 13.

[22] Uttar Pradesh District Profile. (2015, 08 10). Retrieved August Monday, 2015, from http://zpdk.org.in/sites/default/files/di strictprofile(2-2-10).pdf

[23] Yang, X., Wu, J. J., Shi, P. J., & Yan, F. (2008). Modified triangle method to estimate soil moisture status with moderate resolution imaging spectroradiometer (MODIS) products. The International Archives of the

Photogrammetry, Remote Sensing and Spatial Information Sciences, Vol. XXXVII. Part B8. .